

## SOLUTIONS FOR DISCONTINUOUS BIFURCATION ANALYSIS OF SFRC

**Sonia M. Vrech and Guillermo Etse**

*CONICET, National Scientific and Technical Research Council. CEMNCI, Faculty of Exact Sciences and Engineering, National University of Tucuman, Argentina.*

**Keywords:** Discontinuous bifurcation, failure, SFRC, Mixture Theory.

**Abstract.** In this work, the main properties of the discontinuous bifurcation conditions for Steel Fiber Reinforced Concrete (SFRC) under different scenarios of stress states, fiber contents and directions are derived and evaluated by the spectral properties of the critical localization tensor. A fracture energy-based elastoplastic constitutive theory is considered for the concrete matrix. The contribution of three different phases, i. e. concrete matrix, steel fibers bond-slip and dowel matrix-fibers effects are taken into account through the Mixture Theory. Numerical results demonstrate the appropriate performance of the localization indicator regarding different fiber volumes and distributions.

## 1 INTRODUCTION

The development of innovative composites based on further enhancing of cementitious materials represents a new challenging and interesting field of the Material Science and the Structural Engineering. Most significant examples are the High Performance Concretes and, particularly, the Steel Fiber Reinforced Concrete (SFRC), see a.o. [Gettu \(2008\)](#); [Li et al. \(1998a,b\)](#); [Mirsayah and Banthia \(2002\)](#). Actually, the application of SFRC in civil and military constructions have significantly increased in the last decades (and that trend still continues). The well-known deficiencies of cement-based materials like concretes, i.e., low strength and brittle response in low confinement and tensile regimes, can be mitigated by adding short steel fibers randomly distributed into the cementitious mortar. The major advantages of SFRC, as compared with plain concretes, is its higher residual tensile strength accompanied with elevate toughness in post-cracking regime, see [Naaman and Reinhardt \(2006\)](#); [di Prisco and Plizzari \(2009\)](#); [Nguyen et al. \(2010\)](#). Since fiber bridging mechanisms mainly take place under cracked regime of concrete matrix, the mechanical behavior of uncracked members is practically not influenced by the addition of fibers beyond the limited increase of the elastic stiffness.

In the last years, many constitutive theories were proposed for failure analysis of SFRC. Most of them follow the Smeared Crack Approach (SCA) and, particularly, the flow theory of plasticity, as in the cases of [Hu et al. \(2003\)](#); [Seow and Swaddiwudhipong \(2005\)](#) and the continuum damage theory, see a.o. the work by [Li and Li \(2001\)](#). Besides the SCA-based proposals, several constitutive models and theoretical formulations are based on the Discrete Crack Approach. In this case the kinematic of cracking is modelled by means of the displacement field in discontinuities or interfaces in the finite element discretization, see a.o. the contributions by [Prasad and Krishnamoorthy \(2002\)](#), [Etse et al. \(2012\)](#).

The failure behavior of SFRC was evaluated not only at the macroscopic level of observation but also at the mesoscopic one. We may here refer to the contributions by [Leite et al. \(2004\)](#) and [Schauffert and Cusatis \(2012\)](#) who considered the effect of fibers dispersed into a Lattice Discrete Particle Model, by [Oliver et al. \(2012\)](#) who highlighted the macroscopic response in terms of the meso-structural phenomenon associated with the fiber-matrix bond-slip action, by [Gal and Kryvoruk \(2011\)](#) who proposed a mesoscale two-step homogenization approach and the proposals by [Radtke et al. \(2010\)](#) and [Cunha et al. \(2012\)](#) whereby the SFRC has been considered as a two-phase material. A discrete crack model to predict failure behavior of SFRC based on “Mixture Theory” concepts allowing both macroscopic and mesoscopic analysis has been proposed by the authors in [Etse et al. \(2012\)](#); [Caggiano et al. \(2012\)](#).

The present work formulates a thermodynamically consistent fracture-based model for simulating the failure behavior of SFRC. Fiber effects are taken into account through both a bond-slip formulation and a dowel model. The general basis of the proposed theory for SFRC are presented in Section 2. Section 3 is related to the application of the well-known “Mixture Theory” by [Truesdell and Toupin \(1960\)](#) to describe the mechanical behavior of SFRC, following previous contributions by [Oliver et al. \(2008\)](#) and [Vrech et al. \(2010\)](#). Particularly, Subsection 3.1 reports the constitutive laws featuring the fracture-based softening formulation for plain concrete, while the model description of the fiber-to-concrete interactions, approximating throughout debonding mechanisms and dowel effects of fibers crossing cracks, are highlighted in Subsections 3.2, 3.3 and 3.4. In Section 4 the discontinuous bifurcation condition for SFRC is derived, while in Section 5 the analytical solution for localized failure is evaluated regarding the variation of fiber contents and directions.

## 2 THERMODYNAMICALLY CONSISTENT THEORY

A thermodynamically consistent elasto-plastic constitutive model is proposed for simulating the failure behavior of SFRC. The fundamental assumptions are:

- SFRC as a composite material consisting of three phases: matrix concrete, steel fibers bond-slip and dowel interaction mechanisms;
- according to the Mixture Theory, in every infinitesimal volume the kinematic field of the equivalent continuum and that one of each mixture constituent agree;
- small strains are considered and the rate of the strain tensor is additively decomposed in elastic and plastic components

$$\dot{\boldsymbol{\varepsilon}} = \dot{\boldsymbol{\varepsilon}}^e + \dot{\boldsymbol{\varepsilon}}^p . \quad (1)$$

Under these conditions, at each phase the Helmholtz free energy density can be decomposed into the elastic and plastic components, according to

$$\rho\psi(\boldsymbol{\varepsilon}^e, \kappa) = \rho\psi^e(\boldsymbol{\varepsilon}^e) + \rho\psi^p(\kappa) , \quad (2)$$

where  $\rho$  is the material density and  $\kappa$  the hardening/softening scalar variable, for the case of isotropic plastic behavior. The elastic free energy density is defined as

$$\rho\psi^e(\boldsymbol{\varepsilon}^e) = \frac{1}{2}\boldsymbol{\varepsilon}^e : \mathbf{E}^e : \boldsymbol{\varepsilon}^e \quad , \quad \mathbf{E}^e = \frac{\partial^2\psi^e}{\partial(\boldsymbol{\varepsilon}^e) \otimes \partial(\boldsymbol{\varepsilon}^e)} \quad (3)$$

being  $\mathbf{E}^e$  the fourth-order elastic operator. Regarding Coleman's relations, the constitutive equation for the stress tensor as well as the dissipative stress can be derived from Eq. (2) as

$$\boldsymbol{\sigma} = \rho \frac{\partial\psi^e}{\partial\boldsymbol{\varepsilon}} \quad \text{with} \quad \boldsymbol{\sigma} = \mathbf{E}^e : \boldsymbol{\varepsilon}^e , \quad (4)$$

$$K = -\rho \frac{\partial\psi^p}{\partial\kappa} , \quad (5)$$

respectively, with the dissipation condition

$$D = \boldsymbol{\sigma} : \dot{\boldsymbol{\varepsilon}}^p - K\dot{\kappa} \geq 0 . \quad (6)$$

A convex set of plastically admissible states  $\{(\boldsymbol{\sigma}, K) \leq 0\}$  with the yield function  $F = F(\boldsymbol{\sigma}, K)$  and a dissipative potential  $Q = Q(\boldsymbol{\sigma}, K)$  which turns  $F$  in the case of associated plasticity, are considered. Then, the rate equations for the plastic strains  $\dot{\boldsymbol{\varepsilon}}^p$  and the scalar plastic variable  $\dot{\kappa}$  take the forms

$$\dot{\boldsymbol{\varepsilon}}^p = \dot{\lambda} \frac{\partial Q}{\partial \boldsymbol{\sigma}} \quad \text{and} \quad \dot{\kappa} = \dot{\lambda} \frac{\partial Q}{\partial K} , \quad (7)$$

being  $\dot{\lambda}$  the rate of the plastic parameter.

From the Prandtl–Reuss additive decomposition of the total strain rate tensor into the elastic and plastic components that characterized the flow theory of plasticity in Eq. (1), and considering Eqs. (4) to (7), follow the constitutive equations (in rate form) as

$$\begin{aligned} \dot{\boldsymbol{\sigma}} &= \dot{\boldsymbol{\sigma}}^e - \dot{\lambda} \mathbf{E}^e : \frac{\partial Q}{\partial \boldsymbol{\sigma}} \quad , \quad \dot{\boldsymbol{\sigma}}^e = \mathbf{E}^e : \dot{\boldsymbol{\varepsilon}}^e , \\ \dot{K} &= -\dot{\lambda} H \frac{\partial Q}{\partial K} \quad \text{with} \quad H = \rho \frac{\partial^2\psi^p}{\partial\kappa^2} \end{aligned} \quad (8)$$

being  $H$  the hardening/softening modulus.

The Kuhn–Tucker conditions  $\dot{\lambda} \geq 0$ ,  $F(\boldsymbol{\sigma}, K) \leq 0$ ,  $\dot{\lambda} F(\boldsymbol{\sigma}, K) = 0$ , complete the rate formulation of the Plasticity in terms of hardening variables.

### 3 COMPOSITE CONSTITUTIVE FORMULATION FOR SFRC

In this section, the constitutive formulation for SFRC based on the Mixture Theory by [Truesdell and Toupin \(1960\)](#) is presented. Main assumption of this theory is that in every infinitesimal volume the kinematic field of the equivalent continuum and that one of each mixture constituent, agree. Thus, the stress tensor of the mixture is defined as

$$\boldsymbol{\sigma} = \omega^m \boldsymbol{\sigma}^m + \omega^f \left( \boldsymbol{\sigma}_N^f + \boldsymbol{\sigma}_T^f \right) \quad (9)$$

being  $\omega^m$  and  $\omega^f=1-\omega^m$  the weighting functions depending on the volume fraction of each constituent, with  $m$  and  $f$  referring to concrete matrix and fibers, respectively.  $\boldsymbol{\sigma}_N^f$  and  $\boldsymbol{\sigma}_T^f$  mean the bond-slip and dowel stresses due to the post-cracking interaction between fibers and mortar. These stress components are obtained as the geometrical projection of normal and tangential stresses, respectively. Fiber distribution can be uniform, elliptical, concentrated in one direction or in certain given directions. To this end, the percentage of the total fiber volume in given directions is computed.

#### 3.1 Fracture energy-based thermodynamic model for plain concrete

The fracture energy-based LDP failure criterion by [Vrech and Etse \(2009\)](#) is adopted, expressed in terms of the normalized first and second Haigh Westergaard stress coordinates  $p^*=I_1/3f'_c$  and  $\rho^*=\sqrt{2J_2}/f'_c$ , being  $f'_c$  the uniaxial compressive strength and  $I_1$  and  $J_2$  the first and second invariants to the stress and deviatoric stress tensors, respectively, as

$$\bar{F}^m(p^*, \rho^*) = \frac{3}{2}p^{*2} + m_0 \left( \frac{\rho^*}{\sqrt{6}} + p^* \right) - c_0 = 0. \quad (10)$$

The calibration of the cohesive and frictional parameters  $c_0$  and  $m_0$ , respectively, in terms of  $f'_c$  and the uniaxial tensile strength  $f'_t$ , leads to  $c_0=1$  and  $m_0=3(f'_c - f'_t)/(2f'_c f'_t)$ .

The yield surfaces in the hardening and softening regimes are encompassed by the following one single equation

$$F^m(p^*, \rho^*, K_h, K_s) = \frac{3}{2}p^{*2} + m_0 \left( \frac{\rho^*}{\sqrt{6}} + p^* \right) - K_h K_s = 0. \quad (11)$$

Its evolution in the pre-peak regime is controlled by the variation of the hardening dissipative stress  $0.1 \leq K_h < 1$ , while the softening dissipative stress remains constant  $K_s = 1$ . When  $K_h = 1$ , the LDP criterion is reached. Under monotonic loading beyond peak stress the softening regime is activated. The strength degradation during the post-peak process is controlled by the decay of the softening dissipative stress  $1 > K_h \geq 0$  while  $K_h = 1$  remains constant. Evolution laws for dissipative stresses can be found in [Vrech et al. \(2016\)](#).

The adopted non-associated plastic flow is based on a volumetric modification of the yield condition, resulting

$$Q^m(p^*, \rho^*, K_h, K_s) = F^m(p^*, \rho^*, K_h, K_s) - m_0 p^* (\eta - 1) \quad (12)$$

being  $\eta$  the volumetric non-associativity parameter that varies between  $0 \leq \eta \leq 1$ . The extreme case when  $\eta = 0$  corresponds to the isochoric plastic flow, while  $\eta = 1$  results in associated plasticity.

### 3.2 Thermodynamically consistent crack-bridging effects of fibers crossing cracks

Steel fibers crossing active opened cracks, bring relevant bridging effects on the overall SFRC post-peak toughness. In this work, the bond-slip mechanism between fibers and concrete matrix is taken into account by means of the axial (tensile) fiber stress  $\sigma_N^f$ . Besides, the dowel effect is considered as a shear transfer mechanism within active cracks, by  $\sigma_T^f$ . Simple one-dimensional thermodynamically consistent elasto-plastic constitutive models are proposed in the followings subsections for both interaction mechanisms.

### 3.3 One-dimensional thermodynamic bond-slip model

The proposed elasto-plastic bond-slip constitutive model is defined by means of the following equations

$$\begin{aligned}\psi_N^f &= \frac{1}{2}E^f \left(\varepsilon_N^{f,e}\right)^2 + \frac{1}{2}H_N^f \left(\kappa_N^f\right)^2 && \text{(Free-energy potential)} \\ \sigma_N^f &= E^f (\varepsilon_N^{f,e} - \varepsilon_N^{f,p}) && \text{(Constitutive relation)} \\ \Phi_N^f &= |\sigma_N^f| - (\sigma_y^f + K_N^f) \leq 0 && \text{(Yield function)} \\ \dot{\kappa}_N^f &= \dot{\lambda} && \text{(Internal variable evolution)} \\ \dot{K}_N^f &= H_N^f \dot{\kappa}_N^f && \text{(Softening law)}\end{aligned}\tag{13}$$

where  $\varepsilon_N^{f,e}$  and  $\varepsilon_N^{f,p}$  are the elastic and plastic axial strains, respectively,  $E^f$  the elastic module,  $\sigma_y^f$  the equivalent yield stress and  $H_N^f$  the hardening/softening parameter; whereas  $\kappa_N^f$  is the internal variable, conjugated to the dissipative stress  $K_N^f$ .

According to [Oliver et al. \(2008\)](#), slipping-fibers and fiber-concrete interfaces define a serial system, whereby the fiber total strain  $\varepsilon_N^f$  is assumed as the sum of the proper fiber deformation  $\varepsilon^d$  and the interface sliding  $\varepsilon^i$ ,  $\varepsilon_N^f = \varepsilon^d + \varepsilon^i$ . Whereas the fiber stress  $\sigma_N^f$  is identical on each component  $\sigma_N^f = \sigma_N^d = \sigma_N^i$ . The material mechanical features of this serial system defining the considered bond-slip model result

$$\begin{aligned}E^f &= \frac{1}{1/E^d + 1/E^i} \\ \sigma_y^f &= \min[\sigma_y^d, \sigma_y^i] \\ H_N^f &= \begin{cases} H_N^d, & \text{if } \sigma_y^d < \sigma_y^i \\ H_N^i, & \text{otherwise} \end{cases}\end{aligned}\tag{14}$$

where the superscripts  $d$  and  $i$  denote fiber and interface, respectively.

A complete pull-out analysis of a single fiber has been carried out by [Vrech et al. \(2016\)](#), where the bond response of the fiber-concrete joint depending on the slip developed throughout the embedment length are reported. Different states of the bond response have been also defined, assuming fully elastic behavior of fibers:

- elastic;
- elastic-softening;
- softening;
- elastic-softening debonding;
- softening debonding; and
- debonding failure.

### 3.4 Constitutive model for fiber dowel effect

The following one-dimensional elasto-plastic formulation is considered to take into account the dowel effect of fibers crossing open cracks in cementitious matrix.

The thermodynamically consistent constitutive model proposed in this work is based on the following equations

$$\begin{aligned}
 \psi_T^f &= \frac{1}{2} G^f \varepsilon_T^{f,e} \cdot \varepsilon_T^{f,e} + \frac{1}{2} H_T^f \left( \kappa_T^f \right)^2 && \text{(Free-energy potential)} \\
 \sigma_T^f &= G^f (\varepsilon_T^{f,e} - \varepsilon_T^{f,p}) && \text{(Constitutive relation)} \\
 \Phi_T^f &= |\sigma_T^f| - (\tau_y^f + K_T^f) \leq 0 && \text{(Yield function)} \\
 \dot{\kappa}_T^f &= \dot{\lambda} && \text{(Internal variable evolution)} \\
 \dot{K}_T^f &= H_T^f \dot{\kappa}_T^f && \text{(Softening law)}
 \end{aligned} \tag{15}$$

being  $\varepsilon_T^{f,e}$  and  $\varepsilon_T^{f,p}$  the elastic and plastic shear strain, respectively,  $\kappa_T^f$  the internal variable conjugated to the dissipative stress  $K_T^f$  and  $H_T^f$ , once again, the hardening/softening parameter. The adopted dowel stiffness  $G_f$  and the equivalent strength  $\tau_y^f$  characterizing the dowel mechanism, are based on the definition of both stiffness and strength of a generic fiber embedded in a concrete matrix and subjected to a transverse force. This formulation is developed in analogy to a “semi-infinite” beam on a Winkler foundation following the empirical work by [El-Ariss \(2007\)](#) and the experimental contributions by [Dulacska \(1972\)](#).

## 4 ANALYTICAL SOLUTION FOR LOCALIZED FAILURE

In the framework of the smeared crack approach, localized failure modes are related to discontinuous bifurcations of the equilibrium path, and lead to lost of ellipticity of the equations that govern the static equilibrium problem. The inhomogeneous or localized deformation field exhibits a plane of discontinuity that can be identified by means of the eigenvalue problem of the acoustic or localization tensor, see [Ottosen and Runesson \(1991\)](#). Analytical solutions for the discontinuous bifurcation condition, based on original works by [Hadamard \(1903\)](#), [Thomas \(1961\)](#) and [Hill \(1962\)](#), conduce to the macroscopic localization condition

$$\det(\mathbf{Q}^{ep}) = 0 \tag{16}$$

being  $\mathbf{Q}^{ep}$  the elasto-plastic localization tensor, defined as

$$\mathbf{Q}^{ep} = \mathbf{N} \cdot \mathbf{E}^{ep} \cdot \mathbf{N} \tag{17}$$

with  $\mathbf{N}$ , the normal direction to the discontinuity surface. The elasto-plastic tangent operator can be obtained as

$$\mathbf{E}^{ep} = \mathbf{E}^e - \frac{1}{h} \mathbf{E}^e : \frac{\partial \mathbf{Q}}{\partial \boldsymbol{\sigma}} \otimes \frac{\partial F}{\partial \boldsymbol{\sigma}} : \mathbf{E}^e, \tag{18}$$

whereby the generalized plastic modulus  $h$  is defined as

$$h = \frac{\partial F}{\partial \boldsymbol{\sigma}} : \mathbf{E}^e : \frac{\partial \mathbf{Q}}{\partial \boldsymbol{\sigma}} + H. \tag{19}$$

The localized failure condition of Eq. (16) leads to the analysis of the spectral properties of the localization tensor  $\mathbf{Q}^{ep}$ , that can also be written as

$$\mathbf{Q}^{ep} = \mathbf{Q}^e - \frac{1}{h} \mathbf{a}^* \otimes \mathbf{a}, \tag{20}$$

being  $\mathbf{Q}^e$  the elastic localization tensor

$$\mathbf{Q}^e = \mathbf{N} \cdot \mathbf{E}^e \cdot \mathbf{N} \quad (21)$$

and the vectors  $\mathbf{a}$  and  $\mathbf{a}^*$  defined as

$$\mathbf{a} = \frac{\partial F}{\partial \boldsymbol{\sigma}} : \mathbf{E}^e \cdot \mathbf{N} \quad , \quad \mathbf{a}^* = \mathbf{N} \cdot \mathbf{E}^e : \frac{\partial Q}{\partial \boldsymbol{\sigma}} \quad (22)$$

Then, the smallest autovalue of  $\mathbf{Q}^{ep}$  with respect to the metric defined by  $(\mathbf{Q}^e)^{-1}$  is

$$\lambda^{(1)} = 1 - \frac{\mathbf{a}(\mathbf{N}) \cdot [\mathbf{Q}(\mathbf{N})]^{-1} \cdot \mathbf{a}^*(\mathbf{N})}{h} = 0 \quad (23)$$

By replacing Eqs. (19) and (22) in (23), results the localization condition

$$H_c + \frac{\partial F}{\partial \boldsymbol{\sigma}} : \mathbf{E}^e : \frac{\partial Q}{\partial \boldsymbol{\sigma}} - \mathbf{a} \cdot [\mathbf{Q}(\mathbf{N})]^{-1} \cdot \mathbf{a}^* = 0 \quad (24)$$

that serves as a basis for analytical and numerical evaluations of the most critical (maximum) hardening parameter  $H_c = \max[H_c(\mathbf{N})]$  for discontinuous bifurcation and of their associated localization directions  $\mathbf{N}$ .

## 5 NUMERICAL ANALYSIS OF THE DISCONTINUOUS BIFURCATION CONDITION

In this section, the critical condition for localized failure in the form of discontinuous bifurcation of Eq. (16) is evaluated for plain concrete and SFRC by means of numerical analysis with the proposed model. Main purpose of this analysis is, on one hand, to evaluate the effect of steel fibers on the performance of the localization indicator or on the potential critical directions for localized failure. On the other hand, this analysis allows to evaluate the sensitivity of the fiber orientation on the critical condition for discontinuous bifurcation.

The uniaxial tensile tests by Abrishambaf et al. (2015) is considered. Corresponding material properties are summarized in Table 1, while numerical predictions of the tensile stress-crack width relationship for SFRC have been shown by Vrech et al. (2016).

The performance of the determinant of the normalized localization indicator  $\det(\mathbf{Q}) = \det(\mathbf{Q}^{ep}) / \det(\mathbf{Q}^e)$  at peak and residual stress states of the uniaxial tensile test are shown in Figures 1 and 2, respectively. Plain concrete, as well as SFRC with  $\omega^f = 7\%$  and five different distributions of fiber orientations. The results demonstrate that fiber contribution suppresses the localization condition at peak stress state, in contrast with the plain concrete failure behaviour. On the other hand, according to Figure 2, at residual stress states the localization condition is satisfied by both, plain concrete and SFRC, when debonding failure also occurs. The proposed constitutive theory is able to capture the effect of the fiber orientation on the elastic properties degradation, not only regarding the amount of the degradation but also its orientation. This is a relevant characteristic of the proposed material theory.

## 6 CONCLUSIONS

A thermodynamically consistent elasto-plastic constitutive theory aimed at predicting the failure behavior of SFRC has been presented. The model formulation, founded on a macroscopic smeared crack approach and, particularly, on the full thermodynamic consistency, considers the well-known Mixture Theory to account for the presence of fibers in concrete matrix.

Table 1: Characterization of material properties by Abrishambaf et al. (2015).

Concrete properties	
Elasticity modulus – $E^m$ [GPa]	34.15
Poisson modulus – $\nu$	0.2
Compressive strength – $f'_c$ [MPa]	47.7
Tensile strength – $f'_t$ [MPa]	5.0
Non – associativity parameter – $\eta$	0.5
Steel fibers properties	
Elasticity modulus – $E^d$ [GPa]	200.0
Yield stress – $\sigma_y^d$ [MPa]	1100.0
Equivalent shear elastic modulus – $G^f$ [GPa]	15.0
Equivalent shear strength – $\tau_y^f$ [MPa]	441.67
Hardening/Softening moduli – $H_N^f = H_T^f$	0.0
Fiber – concrete interfaces properties	
Elasticity modulus – $E^i$ [GPa]	200.0
Yield stress – $\sigma_y^i$ [MPa]	198.0

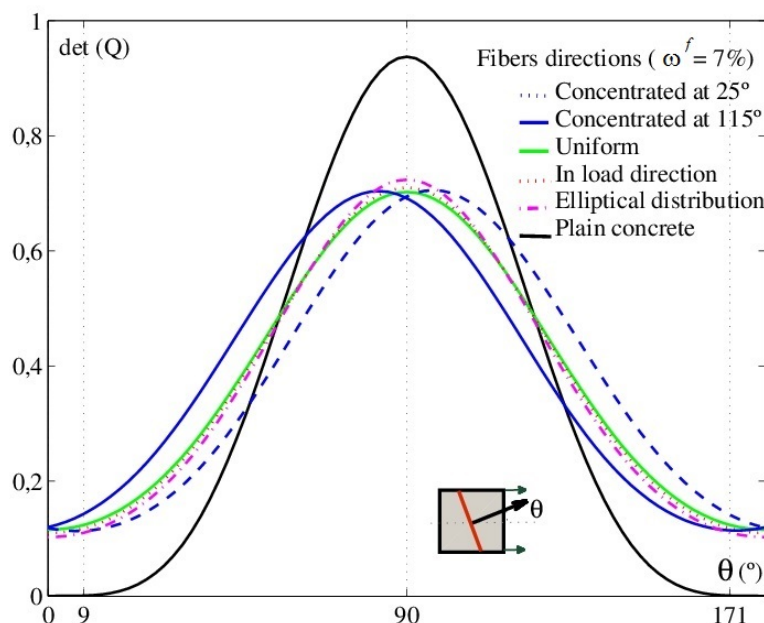


Figure 1: Numerical localization analysis at peak of the uniaxial tensile test.

The model also accounts for bridging interactions of fibers in concrete cracks in the form of fiber-to-concrete bond-slip and dowel mechanisms.

The discontinuous bifurcation conditions for SFRC has been derive by the analysis of the spectral properties of the critical localization tensor and numerically evaluated. A distinguish feature of the proposed constitutive theory is its ability to evaluate non-homogeneous fiber distributions in the concrete matrix and moreover, their effect on both the post-peak load–displacement behavior and the orientation evolution of the critical localization direction in the form of discontinuous bifurcation.

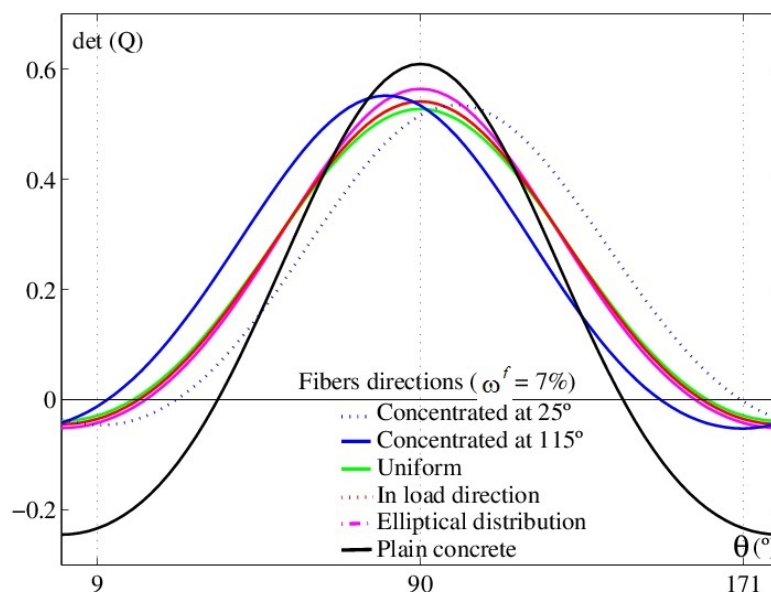


Figure 2: Numerical localization analysis at residual stress state of the uniaxial tensile test.

## ACKNOWLEDGEMENTS

The authors acknowledges the financial support for this work by CONICET (National Council of Scientific and Technical Research, Argentina) through the Grant No. PIP 11220170100795CO and by SCAIT (Secretariat of Science, Art and Technological Innovation of the University of Tucumán, Argentina) through the Grant PIUNT No. E 571.

## REFERENCES

- Abrishambaf A., Barros J., and Cunha V. Tensile stress-crack width law for steel fibre reinforced self-compacting concrete obtained from indirect (splitting) tensile tests. *Cement & Concrete Composites*, 57:153–165, 2015.
- Caggiano A., Etse G., and Martinelli E. Zero-thickness interface model formulation for failure behavior of fiber-reinforced cementitious composites. *Computers & Structures*, 98-99:23–32, 2012.
- Cunha V., Barros J., and Sena-Cruz J. A finite element model with discrete embedded elements for fibre reinforced composites. *Computers & Structures*, 94-95:22–33, 2012.
- di Prisco M. and Plizzari G. and Vandewalle L. Fiber reinforced concrete: new design perspectives. *Materials and Structures*, 42:1261–1281, 2009.
- Dulacska H. Dowel action of reinforcement crossing cracks in concrete. *ACI Structural J*, 69(12):754–757, 1972.
- El-Ariss B. Behavior of beams with dowel action. *Engrg Structures*, 29(6):899–903, 2007.
- Etse G., Caggiano A., and Vrech S. Multiscale failure analysis of fiber reinforced concrete based on a discrete crack model. *Int J of Fracture*, 178(1-2):131–146, 2012.
- Gal E. and Kryvoruk R. Meso-scale analysis of FRC using a two-step homogenization approach. *Computers & Structures*, 89(11-12):921–929, 2011.
- Gettu R. *Fiber Reinforced Concrete: design and applications*. BEFIB 2008, Bagnaux, France, RILEM Publications S.A.R.L., PRO60, 2008.
- Hadamard J. *Propagation des ondes et les equations d'Hydrodynamique*. New York. Chelsea,

- 1903.
- Hill R. Acceleration waves in solids. *J. Mech. of Phys. and Sol.*, pages 1–16, 1962.
- Hu X., Day R., and Dux P. Biaxial failure model for fiber reinforced concrete. *J of Materials in Civil Engrg*, 15(6):609–615, 2003.
- Leite J., Slowik V., and Mihashi H. Computer simulation of fracture processes of concrete using mesolevel models of lattice structures. *Cement and Concrete Research*, 34(6):1025–1023, 2004.
- Li F. and Li Z. Continuum damage mechanics based modeling of fiber reinforced concrete in tension. *International Journal of Solids and Structures*, 38(5):777–793, 2001.
- Li V., Lin Z., and Matsumoto T. Influence of fiber bridging on structural size-effect. *International Journal of Solids and Structures*, 35:4223–4238, 1998a.
- Li Z., Li F., Chang T., and Mai Y. Uniaxial tensile behavior of concrete reinforced with randomly distributed short fibers. *ACI Mat J*, pages 564–574, 1998b.
- Mirsayah A. and Banthia N. Shear strength of steel fiber-reinforced concrete. *ACI Mat J*, 5:473–479, 2002.
- Naaman A. and Reinhardt H. Proposed classification of HPFRC composites based on their tensile response. *Materials and Structures*, 39:547–555, 2006.
- Nguyen A., Stoffel M., and Weichert D. A one-dimensional dynamic analysis of strain-gradient viscoplasticity. *Europ J of Mechanics - A/Solids*, 2(6):1042–1050, 2010.
- Oliver J., Linero D.L., Huespe A., and Manzoli O. Two-dimensional modeling of material failure in reinforced concrete by means of a continuum strong discontinuity approach. *Computer Methods in Applied Mechanics and Engrg*, 197:332–348, 2008.
- Oliver J., Mora D., Huespe A., and Weyler A. A micromorphic model for steel fiber reinforced concrete. *Int J of Solids and Structures*, 197:2990–3007, 2012.
- Ottosen S. and Runesson K. Properties of discontinuous bifurcation solutions in elasto-plasticity. *International Journal of Solids and Structures*, 27:401–421, 1991.
- Prasad M. and Krishnamoorthy C. Computational model for discrete crack growth in plain and reinforced concrete. *Computer Methods in Applied Mechanics and Engrg*, 191(25-26):2699–2725, 2002.
- Radtke F., Simone A., and Sluys L. A computational model for failure analysis of fiber reinforced concrete with discrete treatment of fibers. *Engrg Fracture Mechanics*, 77(4):597–620, 2010.
- Schauffert E. and Cusatis G. Lattice discrete particle model for fiber reinforced concrete (LDPM-F). I: Theory. *J of Eng Mech*, 138(7):826–833, 2012.
- Seow P. and Swaddiwudhipong S. Failure surface for concrete under multiaxial load - a unified approach. *J of Materials in Civil Engrg*, 17(2):219–228, 2005.
- Thomas T. *Plastic flow and fracture in solids*. Academic Press, London, 1961.
- Truesdell C. and Toupin R. *The classical field theories. Handbuch der Physik*. Springer-Verlag, Berlin III/I, 1960.
- Vrech S. and Etse G. Gradient and fracture energy-based plasticity theory for quasi-brittle materials like concrete. *Comput. Methods Appl. Mech. Engrg.*, 199:136–147, 2009.
- Vrech S., Etse G., and Caggiano A. Thermodynamically consistent elasto-plastic microplane formulation for fiber reinforced concrete. *International Journal of Solids and Structures*, 81:337–349, 2016.
- Vrech S., Etse G., Meschke G., Caggiano A., and Martinelli E. *Meso- and macroscopic models for fiber-reinforced concrete*. Computational Modelling of Concrete Structures, Rohrmoos/Schladming, Austria, 2010.